

Stereochemistry in the Reaction of the *myo*-Inositol Phosphate Synthase Ortholog Ari2 during Aristeromycin Biosynthesis

Fumitaka Kudo,* Takeshi Tsunoda, Kaito Yamaguchi, Akimasa Miyanaga, and Tadashi Eguchi*

Department of Chemistry, Tokyo Institute of Technology, 2-12-1, O-okayama, Meguro-ku, Tokyo 152-8551, Japan

Corresponding author: *fkudo@chem.titech.ac.jp, *eguchi@chem.titech.ac.jp

Experimental details

General procedure

All commercial reagents derived from TCI, Kanto Chemical and Sigma Aldrich were used as provided unless otherwise indicated. ¹H- and ¹³C-NMR spectra were recorded with a Bruker DRX500 spectrometer or JEOL ECX400 spectrometer. FAB-MS spectra were recorded with a JEOL JMS700 MStation.

Feeding experiments

Streptomyces citricolor NBRC 13005 was maintained on a plate of ISP-2 agar (0.4% yeast extract, 1% malt extract, glucose 0.4%, agar 2.0%, pH was adjusted to 7.3 with NaOH) at 28 °C. D-[6,6-²H₂], (6*S*)-D-[6-²H₁], and (6*R*)-D-[6-²H₁]Glucose were prepared according to the reported method.¹ All of glucose in the ISP-2 medium was replaced with the deuterium labeled glucose for the feeding experiments. Two plates containing 15 mL agar medium (total 30 mL) were used for each feeding experiment. After incubation for 7 days at 28 °C, the solid culture was grinded in mortar with pestle. The grinded culture was then suspended in water and stirred overnight. After centrifugation, the obtained supernatant was loaded on Dowex 50W X-8 (H⁺ form) and washed with water. The bound cationic compounds were eluted with 4 M of NH₄OH and fractionated. The UV-positive fractions were combined and the solvent was evaporated. The residue was dissolved in water and further purified with HPLC system with a Chromaster 5110 Pump (Hitachi), a 996 Photodiode Array Detector (Waters), and a column oven L-7300 (Hitachi) at 40 °C. Senshu Pak ODS SP100, 20ø x 150 mm (Senshu, Japan) with 14% CH₃OH at a flow rate of 4.0 mL/min was used for the first separation. Further, YMC-Triart PFP, 10ø x 150 mm (YMC, Japan) with 14% CH₃OH at a flow rate of 3.0 mL/min was used for the second separation to yield 0.6 mg, 0.5 mg, and 0.8 mg of aristeromycin from D-[6,6-²H₂], (6*S*)-D-[6-²H₁], and (6*R*)-D-[6-²H₁]glucose, respectively. NMR spectra were recorded on a Bruker DRX500 spectrometer. ¹H-NMR spectra were analyzed in D₂O (99.8 atom% enriched, Kanto Chemical) and ²H-

NMR spectra were analyzed in deuterium-depleted water (≤ 1 ppm, ISOTEC). Chemical shifts are reported in ppm relative to the solvent peaks (4.7 ppm for water).

Ari2 reaction analysis

To prepare (6*S*)-D-[6-²H₁] and (6*R*)-D-[6-²H₁]glucose 6-phosphate, 2 mM of (6*S*)-D-[6-²H₁] or (6*R*)-D-[6-²H₁]glucose, 2.5 mM of ATP, 5 U of hexokinase (Sigma) in the 50 mM of Tris buffer (pH 8.5) containing 100 mM of KCl and 6.5 mM of MgCl₂ were reacted at 28°C overnight. The reaction volume was 60 ml that was divided to 12 tubes (5.0 ml each tube). The resultant solution was transferred to the centrifugal filter (Amicon Ultra, 10K) and proteins were removed at 5,000 g for 20 min. The obtained solution was loaded on a DOWEX AG1-X8 column (HCO₂⁻ form, 25 mL), and the column was washed with water (100 mL) and the enzyme reaction product was eluted with 1.5 M of formic acid and fractionated in 10 mL each fraction. After TLC analysis of each fraction with a developing solution H₂O:CH₃OH:CHCl₃ = 1:5:5, several positive fractions with *p*-anisaldehyde stain reagent (R_f = 0.2) were combined and the solvent was removed by rotary evaporator to obtain (6*S*)-D-[6-²H₁]G6P (25.6 mg, 82.1%) and (6*R*)-D-[6-²H₁]G6P (20.8 mg, 66.7%).

Ari2 was prepared according to our previous report.² The Ari2 reactions were conducted under the following conditions: 0.5 mM of (6*S*)-D-[6-²H₁]G6P or (6*R*)-D-[6-²H₁]G6P, 0.1 mM NAD⁺, 1 mM NH₄Cl, 1 mM MgCl₂, 1 U of phosphoglucose isomerase (Sigma) and 25 μM Ari2 at 28 °C overnight. The reaction volume was 70 ml that was divided to 70 tubes (1.0 mL each tube). After incubation, final 5 μM of 2-deoxy-*scyllo*-inosose (2DOI) synthase, BtrC³ was added and incubated further at 28 °C overnight to consume G6P. The resultant solution was transferred to the centrifugal filter (Amicon Ultra, 10K) and proteins were removed at 5,000 g for 20 min. The obtained solution was loaded on a DOWEX AG1-X8 column (HCO₂⁻ form), and the column was washed with water and 0.75 M of formic acid to remove NAD⁺. The enzyme reaction product was then eluted with 1 M of formic acid and fractionated. After TLC analysis of each fraction with a developing solution H₂O:CH₃OH:CHCl₃ = 1:5:5, the positive fractions with *p*-anisaldehyde stain reagent (R_f = 0.2) were combined and the solvent was removed by rotary evaporator to obtain the Ari2 reaction products.

Crystallization, Data Collection and Structural Determination. Ari2 crystals were grown from a 1:1 mixture of a protein solution (10 mg mL⁻¹ in 10 mM Tris-HCl (pH 8.0), 10% glycerol and 1 mM NAD⁺) and a reservoir solution containing 0.4 M NaCl, 0.2 M Tris-HCl (pH 8.0) and 1.0 M sodium citrate using the sitting-drop vapor diffusion method at 5 °C. Prior to collection of the X-ray data, the crystals were soaked in reservoir solution containing 25% (v/v) glycerol as a cryoprotectant and flash-frozen in a stream of liquid nitrogen. The X-ray diffraction data were collected on a beamline AR-NE3A at the Photon Factory (Tsukuba, Japan) and were subsequently indexed, integrated, and scaled using the iMosflm program.^{4,5} The initial phase was determined by molecular replacement using the Molrep program⁶ with the MIPS structure (PDB code: 1GR0)⁷ as a search model. The structural model of Ari2 was manually constructed with Coot.⁸ Refmac⁹ was used for refinement of the structures. The non-crystallographic symmetry was applied as restraints in the refinement. The structural representations were prepared with PyMOL (DeLano Scientific, Palo Alto, CA, USA). The geometries of the final

structure were evaluated using the program MolProbity.¹⁰ The type of metal ion was assigned as Na⁺ based on Metal Binding Site Validation Server.^{11,12} The resulting coordinates and structure factors have been deposited in the Protein Data Bank (PDB code: 6K96).

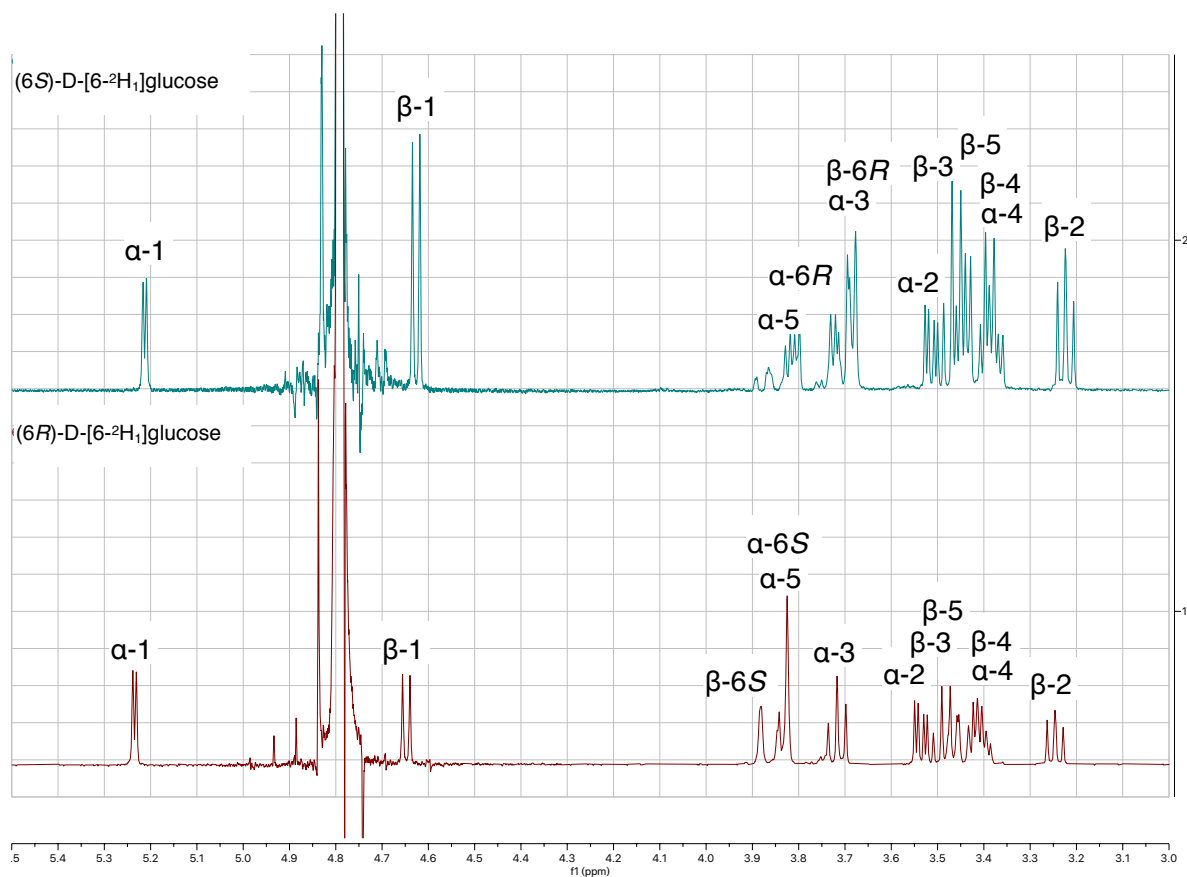
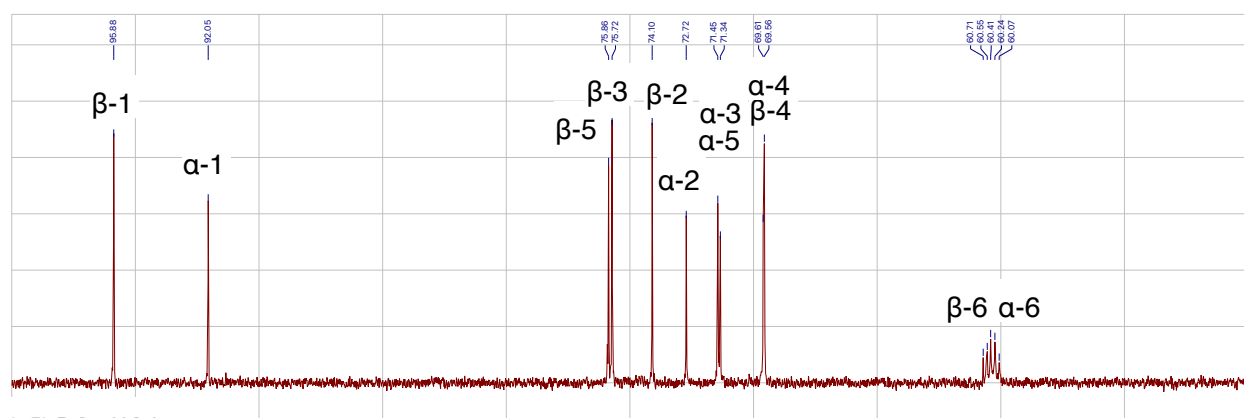


Figure S1. ¹H-NMR of (6*S*)-D-[6-²H₁]glucose and (6*R*)-D-[6-²H₁]glucose (500 MHz, in D₂O).

These data are identical to the ¹H-NMR data of (6*S*)-D-[6-²H₁]glucose and (6*R*)-D-[6-²H₁]glucose in literature.¹

(6*S*)-D-[6-²H₁]glucose



(6*R*)-D-[6-²H₁]glucose

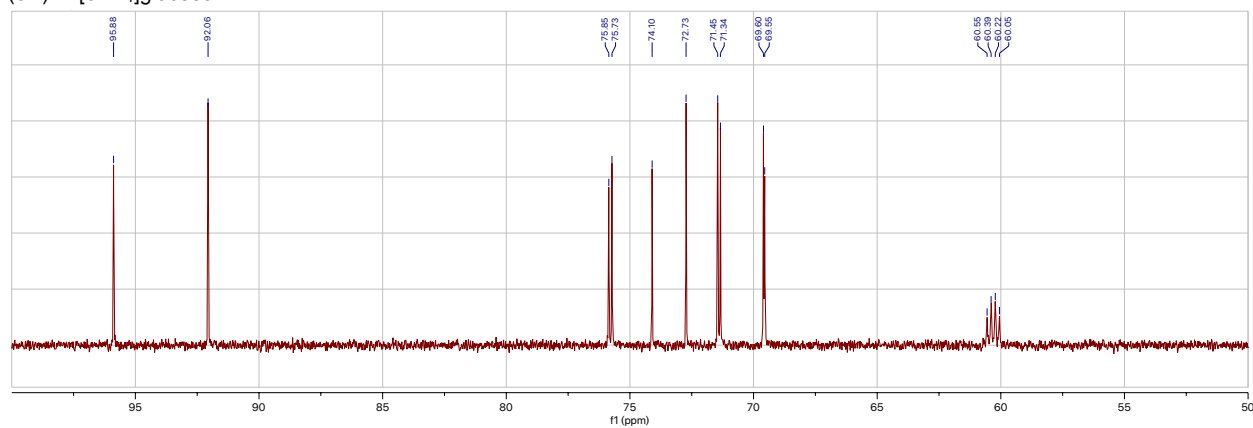


Figure S2. ¹³C-NMR of (6*S*)-D-[6-²H₁]glucose and (6*R*)-D-[6-²H₁]glucose (125 MHz, in D₂O).

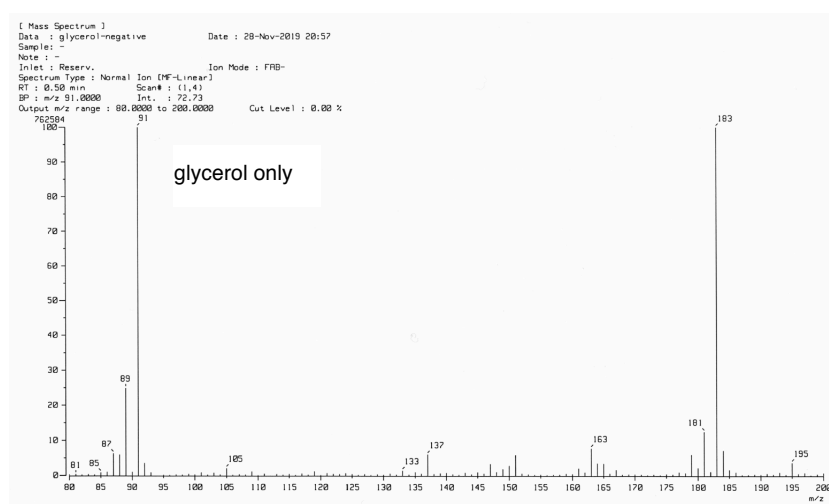
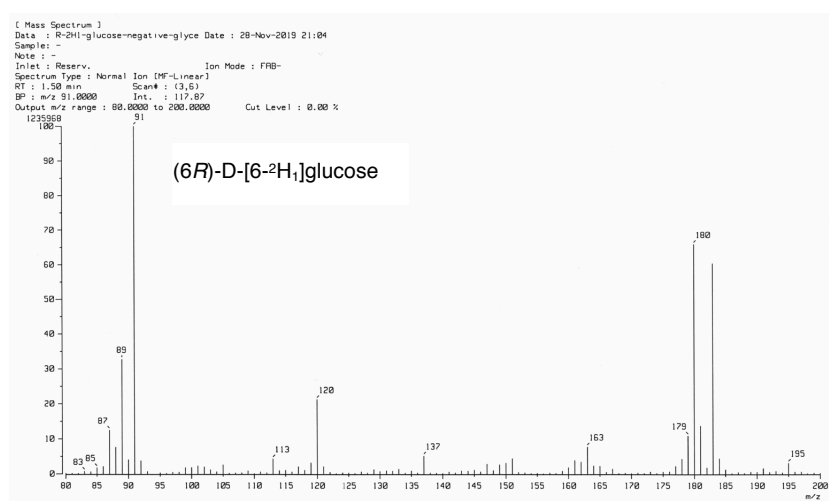
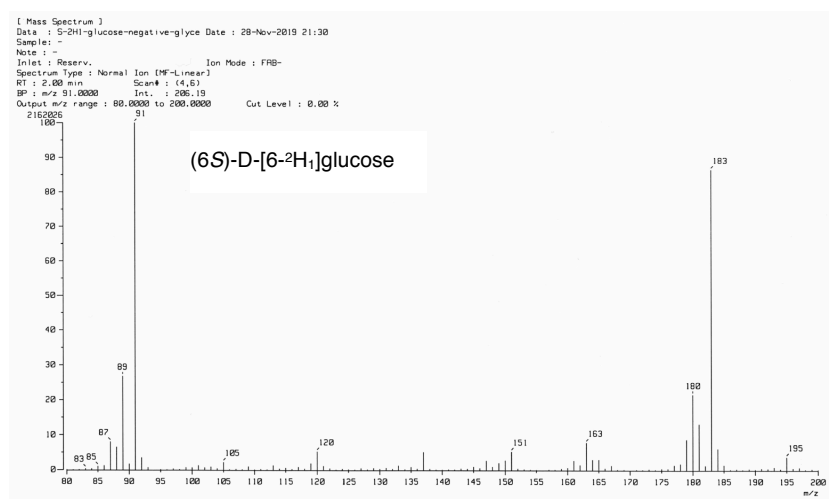


Figure S3. FAB-MS spectra (glycerol matrix, negative mode) of (6S)-D-[6-²H₁]glucose, (6R)-D-[6-²H₁]glucose and glycerol only.

Based on the intensities of *m/z* 179 for non-labeled glucose and *m/z* 180 for mono-deuterium-labeled glucoses, the deuterium enrichment in (6S)-D-[6-²H₁]glucose and (6R)-D-[6-²H₁]glucose were estimated to be approximately 80% and 90%, respectively.

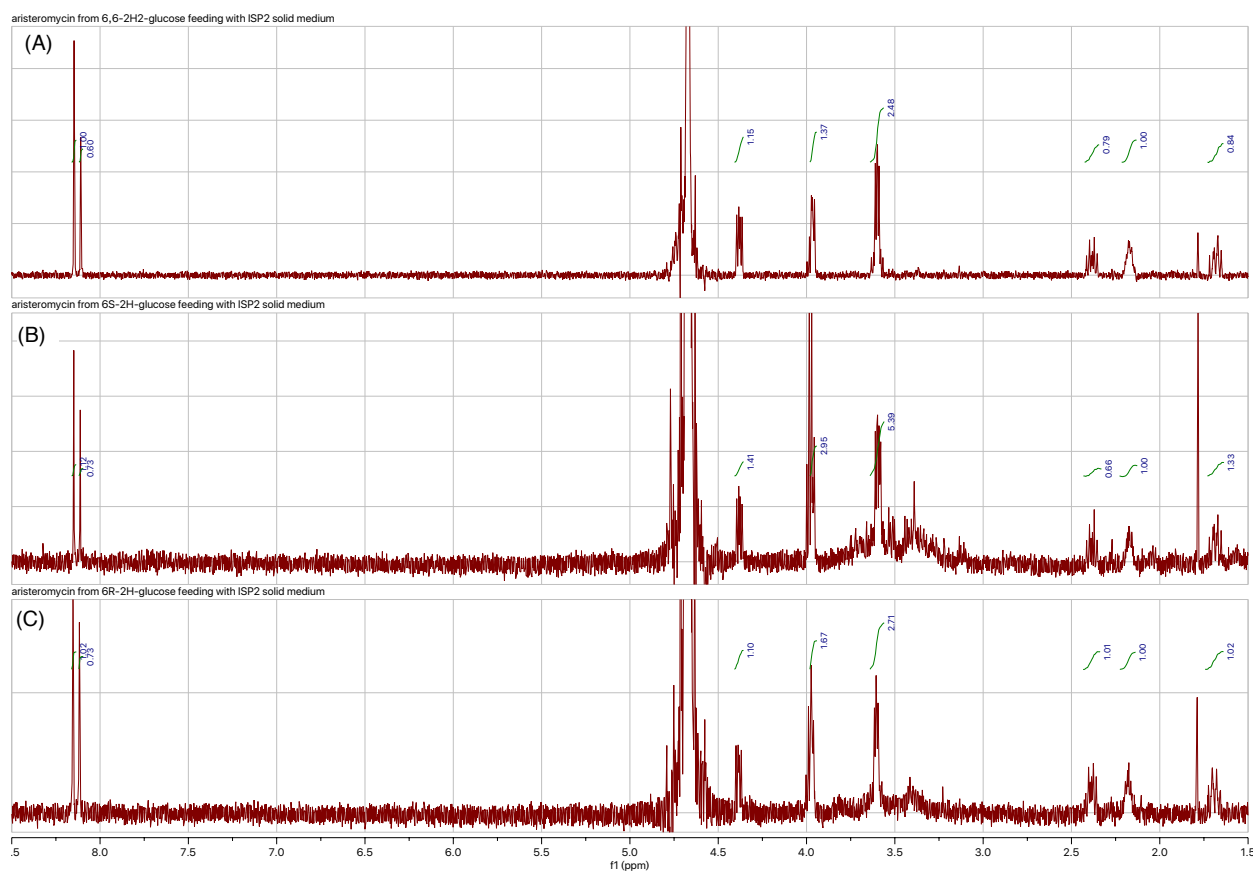


Figure S4. ^1H -NMR of aristeromycins isolated from the solid cultures with D-[6,6- $^2\text{H}_2$]glucose (A), (6S)-D-[6- $^2\text{H}_1$]glucose (B) and (6R)-D-[6- $^2\text{H}_1$]glucose (C) (500 MHz, in D_2O).

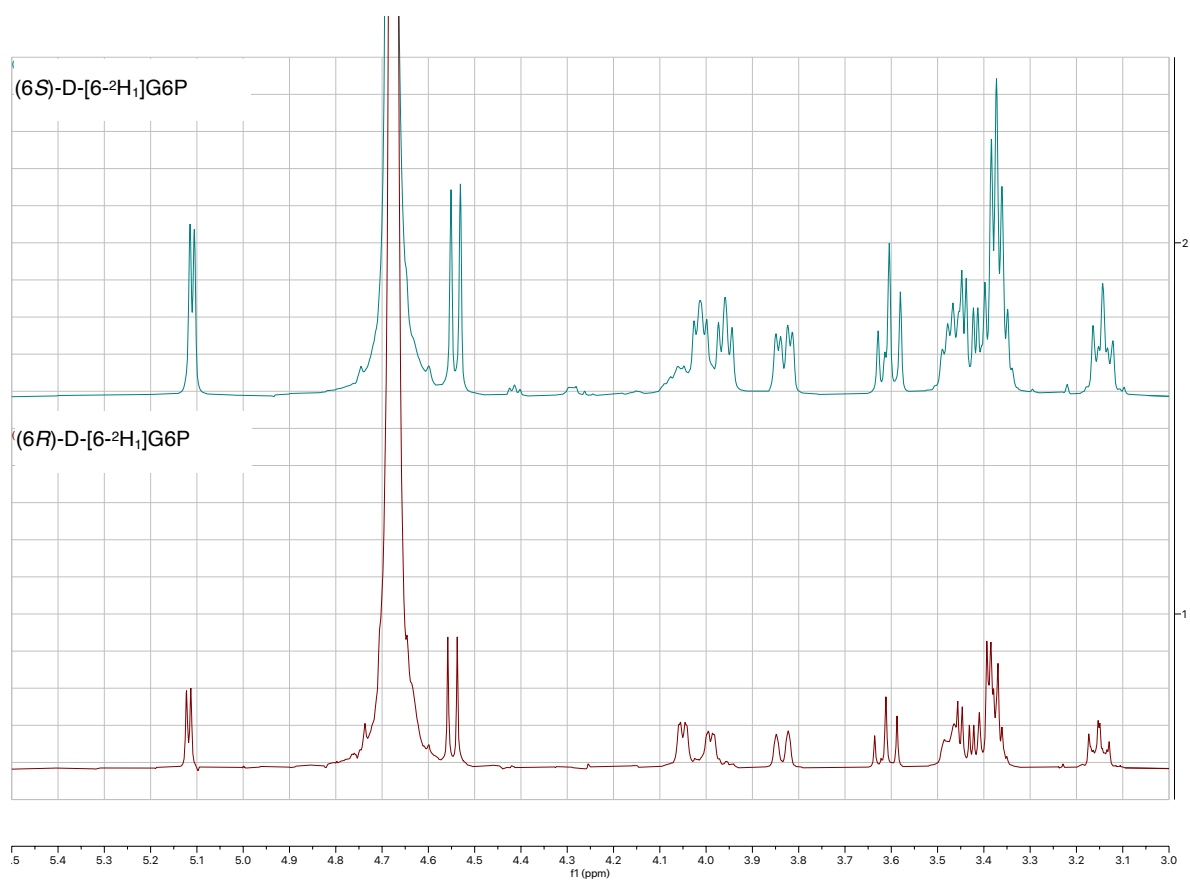


Figure S5. ¹H-NMR of (6*S*)-D-[6-²H₁]G6P and (6*R*)-D-[6-²H₁]G6P (400 MHz, in D₂O).

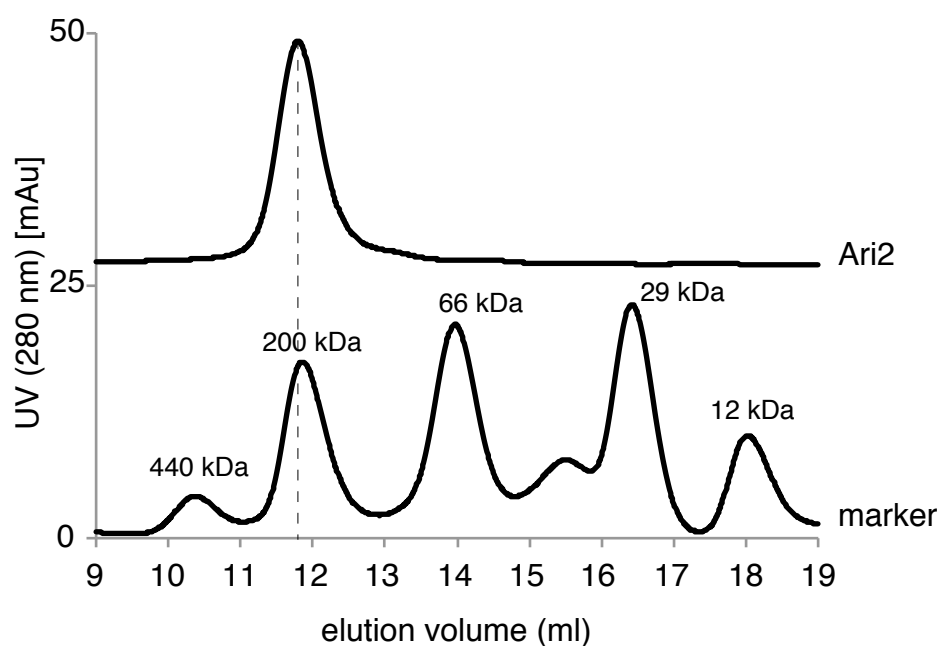


Figure S6. Gel-filtration analysis of Ari2 (38.8 kDa)

Ari2 protein was loaded onto the Superdex 200 10/300 column (GE Healthcare) equilibrated in buffer containing 20 mM HEPES-Na (pH 7.5), 150 mM NaCl and 10% glycerol. Eluted peaks were observed by monitoring the absorbance at 280 nm. Top line: Ari2, Bottom line: molecular weight marker; apoferritin (440 kDa), β -amylase (200 kDa), albumin (66 kDa), carbonic anhydrase (29 kDa), and cytochrome c (12 kDa).

Table S1. Data collection and refinement statistics

Data collection statistics	
Beamline	PF-AR NE-3A
Wavelength (Å)	1.00000
Space group	<i>P</i> 6 ₅ 22
Unit-cell parameters	
<i>a</i> (Å)	101.18
<i>b</i> (Å)	101.18
<i>c</i> (Å)	389.66
Resolution (Å) (outer shell)	50.00–2.50 (2.64–2.50)
Unique reflections	40,934 (5,751)
Redundancy	8.4 (8.7)
Completeness (%)	97.4 (96.3)
<i>R</i> _{merge} (%)	13.8 (40.7)
Mean < <i>I</i> /σ (<i>I</i>)>	12.4 (4.6)
CC _{1/2}	0.990 (0.867)
Refinement statistics	
<i>R</i> _{work} (%)	22.6
<i>R</i> _{free} (%)	28.0
R.m.s. deviations	
Bond lengths (Å)	0.013
Bond angles (°)	1.928
No. of chains in the asymmetric unit	2
No. of non-hydrogen atoms	
Protein	5,048
NAD ⁺	88
Na ⁺	2
Solvent	227
Average B-factors (Å ²)	
Protein	43.1
NAD ⁺	29.7
Na ⁺	26.5
Solvent	44.1
Ramachandran plot	
Favored region (%)	94.9
Allowed region (%)	5.1
Outlier region (%)	0.0

References

- (1) Kakinuma, K. (1984) Synthesis of D-(6*R*)- and D-(6*S*)-(6-²H₁)glucose, *Tetrahedron* **40**, 2089-2094.
- (2) Kudo, F., Tsunoda, T., Takashima, M., and Eguchi, T. (2016) Five-membered cyclitol phosphate formation by a *myo*-inositol phosphate synthase orthologue in the biosynthesis of the carbocyclic nucleoside antibiotic aristeromycin, *ChemBioChem* **17**, 2143-2148.
- (3) Kudo, F., Tamegai, H., Fujiwara, T., Tagami, U., Hirayama, K., and Kakinuma, K. (1999) Molecular cloning of the gene for the key carbocycle-forming enzyme in the biosynthesis of 2-deoxystreptamine-containing aminocyclitol antibiotics and its comparison with dehydroquinase synthase, *J. Antibiot.* **52**, 559-571.
- (4) Battye, T. G., Kontogiannis, L., Johnson, O., Powell, H. R., and Leslie, A. G. (2011) iMOSFLM: a new graphical interface for diffraction-image processing with MOSFLM, *Acta Crystallogr. D Biol. Crystallogr.* **67**, 271-281.
- (5) Powell, H. R., Johnson, O., and Leslie, A. G. (2013) Autoindexing diffraction images with iMosflm, *Acta Crystallogr. D Biol. Crystallogr.* **69**, 1195-1203.
- (6) Vagin, A., and Teplyakov, A. (2010) Molecular replacement with MOLREP, *Acta Crystallogr. D Biol. Crystallogr.* **66**, 22-25.
- (7) Norman, R. A., McAlister, M. S., Murray-Rust, J., Movahedzadeh, F., Stoker, N. G., and McDonald, N. Q. (2002) Crystal structure of inositol 1-phosphate synthase from *Mycobacterium tuberculosis*, a key enzyme in phosphatidylinositol synthesis, *Structure* **10**, 393-402.
- (8) Emsley, P., and Cowtan, K. (2004) Coot: model-building tools for molecular graphics, *Acta Crystallogr. D Biol. Crystallogr.* **60**, 2126-2132.
- (9) Murshudov, G. N., Vagin, A. A., and Dodson, E. J. (1997) Refinement of macromolecular structures by the maximum-likelihood method, *Acta Crystallogr. D Biol. Crystallogr.* **53**, 240-255.
- (10) Chen, V. B., Arendall, W. B., 3rd, Headd, J. J., Keedy, D. A., Immormino, R. M., Kapral, G. J., Murray, L. W., Richardson, J. S., and Richardson, D. C. (2010) MolProbity: all-atom structure validation for macromolecular crystallography, *Acta Crystallogr. D Biol. Crystallogr.* **66**, 12-21.
- (11) Zheng, H., Cooper, D. R., Porebski, P. J., Shabalin, I. G., Handing, K. B., and Minor, W. (2017) CheckMyMetal: a macromolecular metal-binding validation tool, *Acta Crystallogr. D Struct. Biol.* **73**, 223-233.
- (12) Zheng, H., Chordia, M. D., Cooper, D. R., Chruszcz, M., Muller, P., Sheldrick, G. M., and Minor, W. (2014) Validation of metal-binding sites in macromolecular structures with the CheckMyMetal web server, *Nat. Protoc.* **9**, 156-170.
- (13) Xu, G., Kong, L., Gong, R., Xu, L., Gao, Y., Jiang, M., Cai, Y. S., Hong, K., Hu, Y., Liu, P., Deng, Z., Price, N. P. J., and Chen, W. (2018) Coordinated biosynthesis of the purine nucleoside antibiotics aristeromycin and coformycin in actinomycetes, *Appl. Environ. Microbiol.* **84**, e01860-01818.
- (14) Komaki, H., Ishikawa, A., Ichikawa, N., Hosoyama, A., Hamada, M., Harunari, E., Nihira, T., Panbangred, W., and Igarashi, Y. (2016) Draft genome sequence of *Streptomyces* sp. MWW064 for elucidating the rakicidin biosynthetic pathway, *Stand. Genomic Sci.* **11**, 83.
- (15) Bentley, S. D., Chater, K. F., Cerdano-Tarraga, A. M., Challis, G. L., Thomson, N. R., James, K. D., Harris, D.

- E., Quail, M. A., Kieser, H., Harper, D., Bateman, A., Brown, S., Chandra, G., Chen, C. W., Collins, M., Cronin, A., Fraser, A., Goble, A., Hidalgo, J., Hornsby, T., Howarth, S., Huang, C. H., Kieser, T., Larke, L., Murphy, L., Oliver, K., O'Neil, S., Rabinowitsch, E., Rajandream, M. A., Rutherford, K., Rutter, S., Seeger, K., Saunders, D., Sharp, S., Squares, R., Squares, S., Taylor, K., Warren, T., Wietzorrek, A., Woodward, J., Barrell, B. G., Parkhill, J., and Hopwood, D. A. (2002) Complete genome sequence of the model actinomycete *Streptomyces coelicolor* A3(2), *Nature* 417, 141-147.
- (16) Ohnishi, Y., Ishikawa, J., Hara, H., Suzuki, H., Ikenoya, M., Ikeda, H., Yamashita, A., Hattori, M., and Horinouchi, S. (2008) Genome sequence of the streptomycin-producing microorganism *Streptomyces griseus* IFO 13350, *J. Bacteriol.* 190, 4050-4060.
- (17) Jin, X., Foley, K. M., and Geiger, J. H. (2004) The structure of the 1L-*myo*-inositol-1-phosphate synthase-NAD⁺-2-deoxy-D-glucitol 6-(*E*)-vinylhomophosphonate complex demands a revision of the enzyme mechanism, *J. Biol. Chem.* 279, 13889-13895.
- (18) Neelon, K., Roberts, M. F., and Stec, B. (2011) Crystal structure of a trapped catalytic intermediate suggests that forced atomic proximity drives the catalysis of mIPS, *Biophys. J.* 101, 2816-2824.